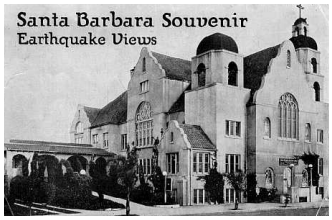

4th IASPEI / IAEE International Symposium:

Effects of Surface Geology on Seismic Motion

August 23–26, 2011 · University of California Santa Barbara

Seismic response of unstable mountain rock slopes: Topographic site effect?

Jan Burjánek
ETH Zürich
Sonneggstrasse 5
8092 Zürich
Switzerland

Jeffrey R. Moore
ETH Zürich
Sonneggstrasse 5
8092 Zürich
Switzerland

Gabriela Gassner-Stamm
ETH Zürich
Sonneggstrasse 5
8092 Zürich
Switzerland

Donat Fäh
ETH Zürich
Sonneggstrasse 5
8092 Zürich
Switzerland

ABSTRACT

As earthquakes are among the main triggers of slope failure, co-seismic landslides contribute significantly to earthquake damage in areas of large topographic relief. Topographic amplification is commonly implicated as a source of augmented ground motion in steep terrain. We performed a number of field experiments to constrain the seismic response of potential future rockslides. We conclude that rather than the shape of topography, amplification due to the internal structure of the instability is of primary importance. Specifically, we deployed small aperture seismic arrays to record ambient vibrations and earthquakes on unstable rock slopes in Swiss Alps. The recordings were analyzed by means of a high resolution *f-k* method, site-to-reference spectral ratios, and time-frequency dependent polarization analysis. The wavefield within the unstable rock mass was found to be dominated by normal modes of individual rock blocks rather than horizontal propagation of seismic waves. The observed amplification is strongly directional, and the maximum amplification is perpendicular to open cracks mapped on the surface. Polarization directions estimated from ambient seismic vibrations are in good agreement with the deformation directions obtained by geodetic and in-situ measurements. No such site effects were observed on stable part of the slopes.

INTRODUCTION

Earthquakes are among the main triggers of landslides, and co-seismic slope failures contribute significantly to earthquake-induced damage in areas of large topographic relief (Marano *et al.*, 2010). Although a number of studies exist on the topic (reviewed by Keefer, 2002), most of these are focused on systematic documentation of past events. Quantitative evaluation of a slope's susceptibility to ground shaking is still typically based on simplified models, which ignore interactions between incoming waves and the topography or internal structure of the landslide. On the other hand, detailed numerical simulation of these phenomena requires a complex geophysical model, which can only be constrained by extensive field investigations at potential slope instabilities (e.g. Danneels *et al.*, 2008; Gischig *et al.*, 2011).

In this paper, we investigate the seismic response of two large, unstable rock slopes by means of array recordings of ambient vibrations and weak earthquakes. We review our recent observations at the two sites and present simplified numerical simulation of observed phenomena. We argue that internal structure plays a predominant role in understanding the seismic response of unstable rock slopes, rather than topography itself.

STUDY AREA

The area of canton Valais is the most seismically active region in Switzerland and home to some of the greatest topographic relief in the Alps. On average, a magnitude 6 earthquake occurs every one hundred years (Fäh *et al.*, 2011). Numerous rock slopes in the Matter valley area have been identified as unstable (Yugsi, 2010), and a number of co-seismic slope collapses have been observed in the past (Fritsche *et al.*, 2006; Fritsche *et al.*, 2010; Fritsche and Fäh, 2009). Since the region is relatively accessible, it has been extensively studied and a solid background of relevant geological information is available (Yugsi, 2010). Therefore, it is favorable for studying seismic triggering of landslides and site effects in unstable, hard-rock slopes.

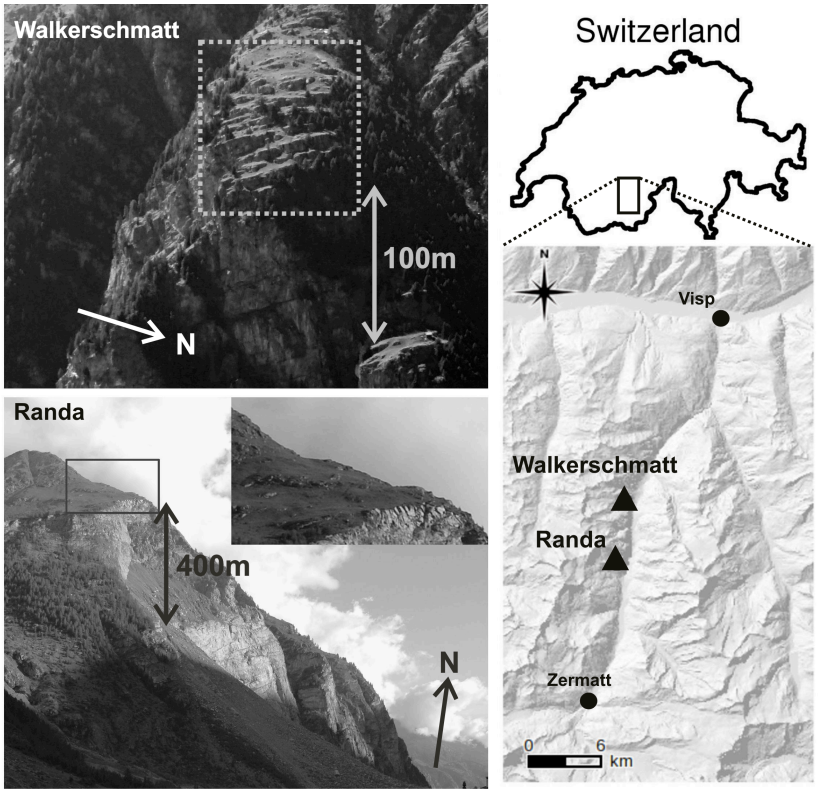

Fig. 1. Photographs of the two study sites and their relative locations within the Matter valley (relief map at right). Seismic stations were deployed in the area marked by rectangles. For the Randa instability, the study site is enlarged in the inset photograph (two plateaus where the arrays were deployed are distinguishable in the zoomed view). The photo also shows the scarp and debris cone of the prominent 1991 rockslides. Vertical scale is roughly represented by the double-headed arrows. The exposed eastern flank of the Matter valley is recognizable from the relief map. The total elevation difference between mountain peaks and the adjacent valley bottom locally exceeds 3000 m.

The first study site discussed in this paper, *Walkerschmatt*, lies on a small topographic bench bounded by steep cliffs near the village of St. Niklaus in the Matter valley (Fig. 1). The potential instability consists of an estimated 0.8 – 1 million m^3 of crystalline rock (Yugsi, 2010). The stepped meadow at the top of the instability is transected by a network of open fractures (sometimes open by 1 m or more) bearing record of past or ongoing deformation (Fig. 1).The second study site, *Randa*, lies 6 km south of Walkerschmatt. The current Randa rock slope instability (Fig. 1) is the legacy of two catastrophic failures in April and May 1991. Around 5 million m^3 of layered paragneiss and schists remain unstable today (the upper half of the 1991 failure scarp), moving at rates up to 20 mm/yr (Gischig *et al.,* 2011). Underlying this unstable rock mass, a steep orthogneiss cliff shows no ongoing deformation after being exposed by the 1991 failures.

FIELD EXPERIMENTS

Both sites under investigation were densely instrumented with seismic stations. The location and type of seismic instruments are indicated in Fig. 2. Data sets acquired at Randa include triggered recordings of regional earthquakes obtained by a micro-seismic monitoring array, continuous recordings from two seismometers located inside and outside of the unstable rock mass, and ambient vibration array surveys. The micro-seismic monitoring network, consisting of three-component geophones with an Eigen-frequency of 8 Hz, recorded 76 regional earthquakes between 2002 and 2004. However, the primary purpose of this network was to monitor seismicity originating within the Randa instability. Subsequent continuous recordings from two seismometers (RAND1 and RAND2) were obtained in 2009 using three-component velocity sensors with an Eigen-period of 5 sec, and contain seismograms of 7 regional earthquakes. Ambient vibration array surveys were performed with the same type of instrument, and lasted one day for each of the two sites. Detailed descriptions of the experiments are provided by Spillmann *et al.* (2007), Burjanek *et al.* (2010), and Burjanek *et al.* (2011). At Walkerschmatt, only ambient vibration array recordings are available.

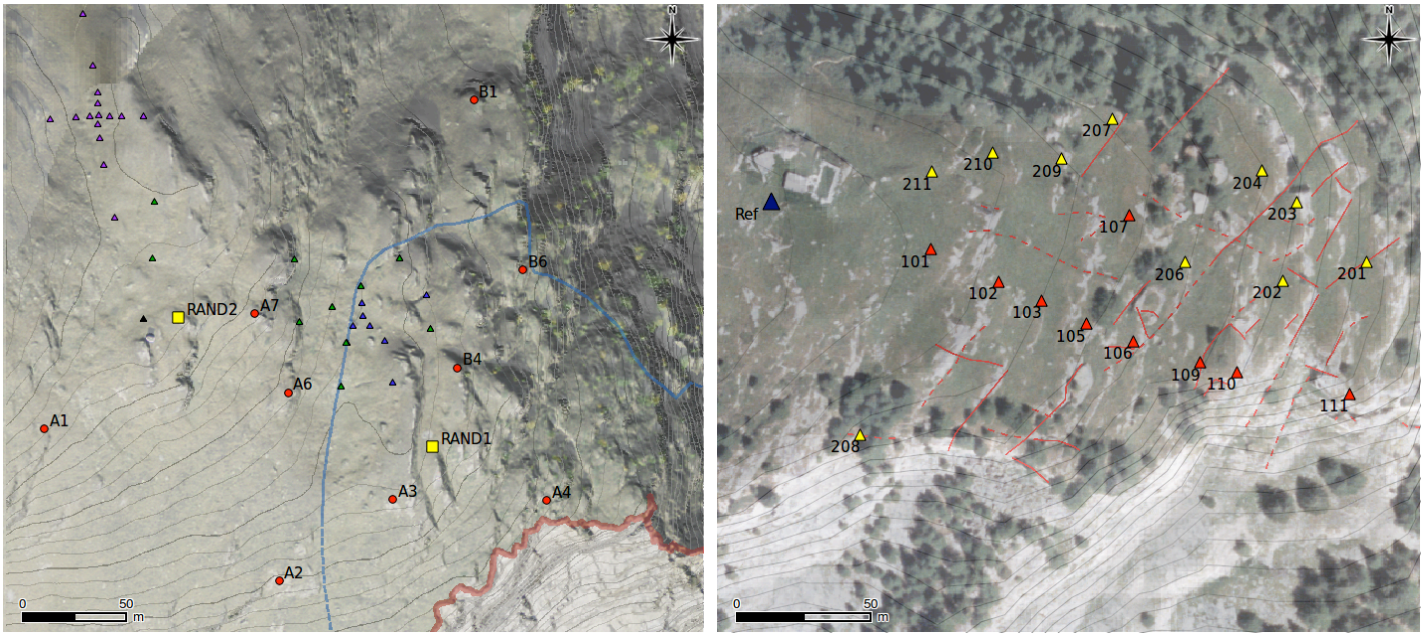

Fig. 2. Layout of seismic arrays. Randa (left): ambient vibration array measurements (triangles), temporary geophone array (circles), and temporary seismometer deployment (squares). The blue line indicates the border of the instability, while the thick brown line marks the scarp of the 1991 rockslide. Walkerschmatt (right): ambient vibration array measurements (triangles); naming convention: e.g., 204 denotes station WAL204. Open cracks mapped at surface are shown as red lines. Stations that were recording simultaneously share the same color (for each of the two sites).

TIME-FREQUENCY POLARIZATION ANALYSIS OF AMBIENT VIBRATIONS

Time-frequency polarization analysis (TFPA) is based on the combination of complex polarization analysis (Vidale, 1986) and the continuous wavelet transform (CWT). The method is described in detail in Burjanek *et al.* (2010), and here we provide only a brief overview. We first use a CWT for signal time-frequency decomposition, and then apply polarization analysis on the complex wavelet amplitude for each time-frequency pair. The particle motion is then characterized for each time and frequency by an ellipse, which is generally tilted in 3-dimensional Euclidean space. Especially the orientation of the major axis and the ellipticity are of primary interest in our analysis. These parameters can be described in the following way: 1) azimuth of the major axis, or strike, measured in degrees from North; 2) tilt of the major axis, or dip, measured in degrees downward from the horizontal; and 3) ellipticity, defined as the ratio between the length of the semi-minor and semi-major axes. All three polarization parameters vary with both time and frequency. The time-frequency resolution is generally controlled by the choice of mother wavelet utilized in the CWT (e.g., Torrence and Compo, 1998). The Morlet mother wavelet, a complex exponential modulated by a Gaussian envelope, was adopted in this study. The time-frequency resolution in this case is then simply controlled by changing the width of the Gaussian envelope.

We assume that observed ambient vibrations are quasi-stationary (i.e. noise properties do not change systematically on the time scale of the experiment – a few hours), and analyze the relative occurrence of polarization parameters. In particular, histograms of polarization parameters were constructed over time for each frequency. Polar plots were then adopted for the presentation of final results, which illustrate combined angular and frequency dependence (Fig. 3, 4). We found that histograms of ellipticity (for a single frequency band) typically resulted in an asymmetric broad peak, which was represented well by a beta distribution. Parameters of the beta distribution could be estimated for each frequency by standard statistical methods (e.g., the maximum likelihood method). In this study, we applied the method-of-moments, where the parameter estimate is based on the sample mean and variance. The estimated mode values are interconnected by a line (e.g., Fig. 4c) to illustrate the variation of ellipticity with frequency. The curve can be considered as a central value, whereas histograms in the background represent the scatter. Since the mode estimate is not based on histograms, it is not affected by the choice of bin width, and smoothly maps the frequency dependence.

The presented method has the advantage of being more generalized than commonly used azimuthally-dependent H/V spectral ratios (e.g., Del Gaudio and Wasowski, 2007; Panzera *et al.*, 2011). A direct comparison of the directional H/V and relative occurrence of azimuth (strike) obtained with TFPA for a common recording of ambient vibrations is presented in Fig. 3. TFPA clearly outperforms directional H/V providing better directional resolution.

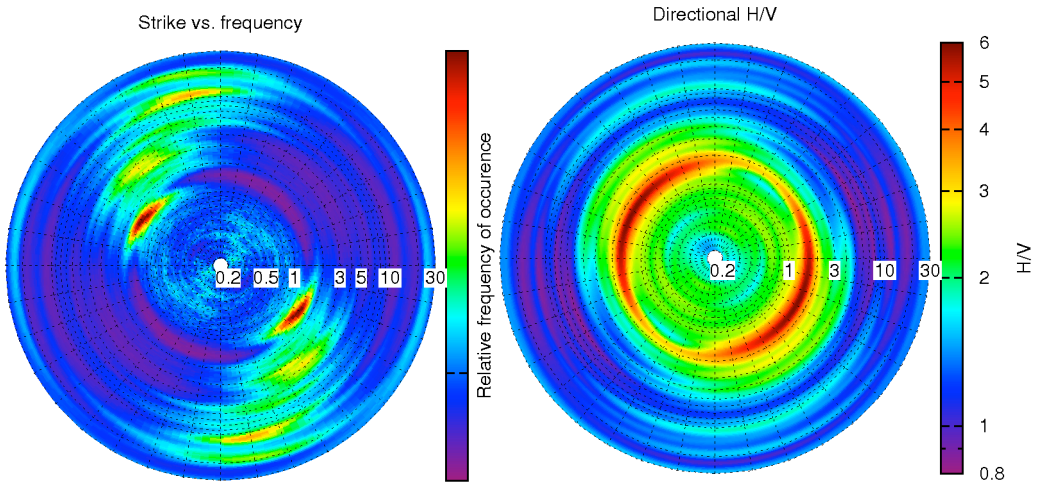

Fig. 3. Comparison of two processing methods of single station three-component ambient vibration measurements. The relative occurrence of strike (azimuth) of ambient vibrations obtained with time-frequency polarization analysis is presented at left. The directional dependent H/V ratio is presented on right. Frequency changes along the radius from 0.2 to 30 Hz as indicated.

Results

All recordings of ambient vibrations for both sites were processed with TFPA. Results for three Walkerschmatt stations (WALref, WAL209, and WAL204) are presented in Fig. 4. The locations of the three selected stations follow the anticipated transition from stable to unstable parts of the rock slope. Here we discuss some polarization features, especially with respect to the instability boundary, and within the context of three frequency bands: 0.2-1 Hz; 1-2 Hz; 2-30 Hz. In the lowest frequency band (0.2-1 Hz), noise polarization follows a roughly northeast-southwest trend (strike ~ 45°), remains primarily in the horizontal plane (dip ~ 0°), and the ellipticity (~ 0.3) does not follow any specific trend with respect to frequency. This same pattern also applies for most other stations. Nevertheless, histograms are relatively scattered for this lowest frequency band, suggesting that even longer recording times may be required for future experiments. In the highest frequency range (2-30 Hz), results vary significantly from station to station, reflecting small-scale geological heterogeneity at the site. Most interesting is the intermediate frequency range (1-2 Hz). The reference station (WALref) shows only weak polarization – relatively flat and broad maxima centered around f=1.6 Hz, strike ~ 130°, dip ~ 10° – and a slight increase in ellipticity (~0.4). Moving downhill to WAL209 (see Fig. 2), the polarization peak becomes more pronounced, shifts slightly (f=1.6 Hz, strike ~ 120°, dip ~ 5°), and a local minimum appears in ellipticity at 1.6 Hz (Fig. 4f). Finally, moving further into the suspected instability at station WAL204, ellipticity drops to almost zero at 1.6 Hz and the peak becomes even more pronounced (f=1.6 Hz, strike ~ 120°, dip ~ 5°). More detailed description can be found in Burjanek *et al.* (2011).

Similar results were identified also at Randa (Burjanek *et al.*, 2010). The intermediate frequency band (3-6 Hz) of ambient vibrations recorded on the unstable part of the slope was polarized in a common direction of 135°, which is in excellent agreement with in-situ deformation measurements (Burjanek *et al.*, 2010). However, it was not possible to pick a single fundamental frequency with TFPA, as it was possible in case of the Walkerschmatt site (f_0=1.6 Hz). This could be due to shorter recoding times, which resulted in limited resolution.

SITE-TO-REFERENCE SPECTRAL RATIOS

Direct comparison of ground motion recordings between sites has proven to be a useful tool in a number of studies investigating local amplification due to site effects. To ensure that the observed variability in ground motion is caused by changes in site conditions only, one has to remove the variability resulting from source directivity and path effects (e.g., Andrews, 1986). If the distance to the source is sufficiently large (compared to the measurement separation), radiation patterns and path effects can be neglected (Borcherdt, 1970). Such comparison is often conducted from earthquake recordings, where the distance to the source is well-constrained. In particular, amplitude spectra of recordings obtained at a site with known conditions (the reference site) are used to normalize spectra calculated at other sites. These so-called site-to-reference spectral ratios (SRSR) then represent frequency-dependent amplification functions with respect to the reference area. In analyses of ambient vibrations, precise sources are generally not known and the distant-source assumption cannot be validated. However, SRSR calculated using noise recordings can still be representative of local site conditions (e.g., Irikura and Kawanaka, 1980; Roten *et al.*, 2006; Roten and Fäh, 2007).

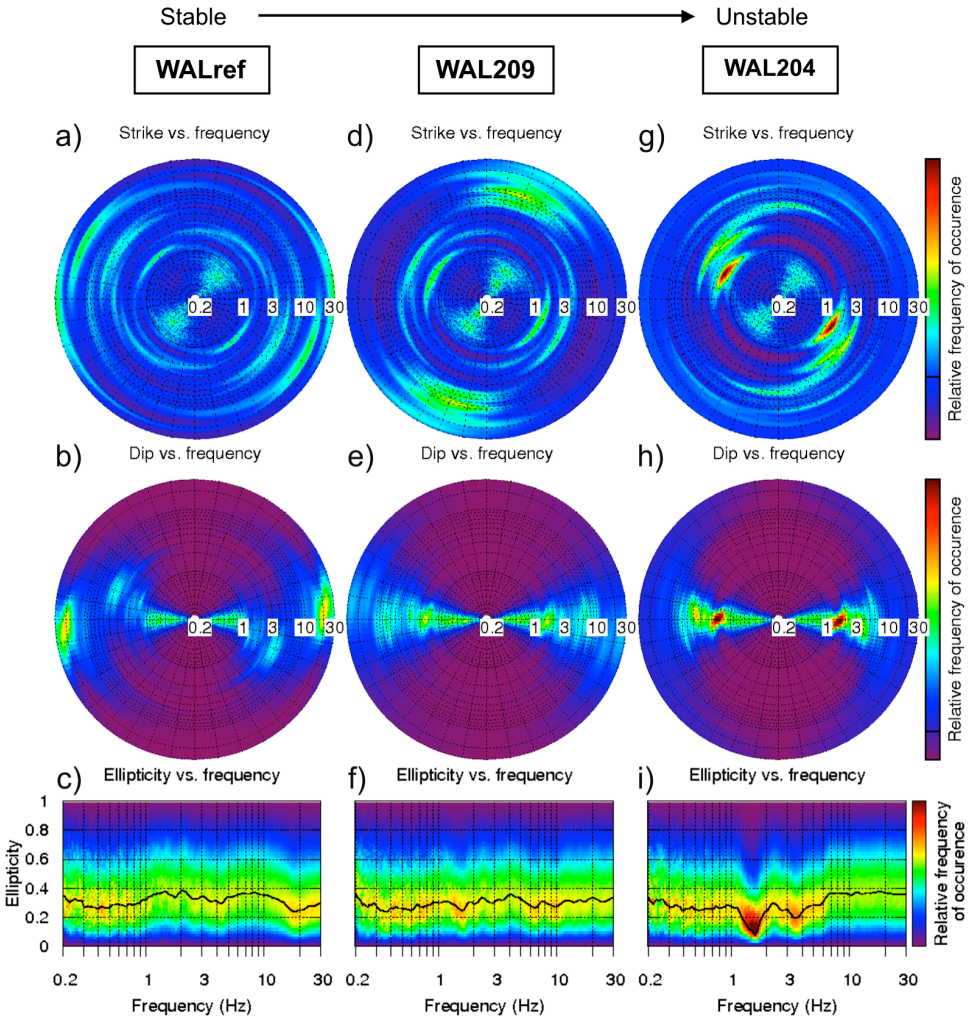

Fig. 4. Results of polarization analysis for three stations at Walkerschmatt: WALref (a-c), WAL209 (d-f), and WAL204 (g-i). Color scale represents the relative frequency of occurrence of strike (a, d, g), dip (b, e, h), and ellipticity (c, f, i). Estimated maxima of the ellipticity distributions (assuming a beta distribution) are connected by the solid black line.

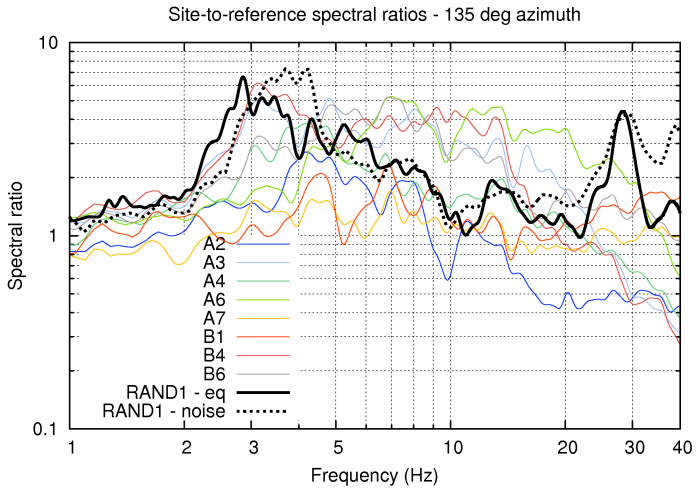

Fig. 5. Mean site-to-reference spectral ratios from Randa. Reference for the micro-seismic array was station A1, station RAND2 served as the reference for RAND1. Site-to-reference ratios were calculated for both earthquake (black solid line) and noise recordings (black dotted line) at station RAND1.

Here we briefly describe the process of the noise SRSR estimation used in the present study. Time series of ambient vibrations were split into 50% overlapping windows of 100 s length and tapered with a cosine window. For each time window, the Fourier amplitude spectrum was calculated and smoothed using the window proposed by Konno and Ohmachi (1998) with bandwidth $b = 40$. Finally the geometrical mean of ratios for all windows was calculated. SRSR based on regional earthquakes were calculated using the S-wave group of the seismogram. The same smoothing was applied as for the noise SRSR analysis.

Results

The micro-seismic monitoring network at Randa site recorded 76 regional earthquakes (M_L ~ 0.5-2) at epicentral distances of 10–40 km. Station A1 (see Fig. 2) located on the stable part of slope was selected as our reference station. Seven additional earthquakes (M_L ~ 0.6-1.6) were recorded by stations RAND1 and RAND2 at epicentral distances 20-40 km. RAND2 served as the reference station for RAND1. Moreover, we estimated SRSR using ambient vibrations (shortly - noise SRSR) at RAND1. Resulting mean site-to-reference spectral ratios are presented in Fig. 5 resolved at an azimuth of 135° (the direction identified by noise polarization analysis). SRSRs show notable amplification within the instability with mean spectral ratios up to ~6. Many stations in the unstable area showed spectral peaks at ~3.1 Hz. Amplification was found to be greatest in the region of maximum instability thickness. Other spectral peaks were identified at frequencies 2.3 Hz (225° azimuth), and 4.7 and 7 Hz (120° azimuth). SRSR for RAND1 is in good agreement with SRSR obtained for the two nearby stations of micro-seismic network (A3, B4), although considerably different instruments were utilized. Finally, noise SRSR is in good agreement with the SRSR obtained from earthquakes for RAND1.

Noise SRSRs for Walkerschmatt were estimated by Burjanek *et al.* (2011). A local maximum of the SRSR (120° azimuth) was observed at 1.6 Hz for all Walkerschmatt stations. Moreover, other local maxima were identified in the calculated spectral ratios (i.e. at 2.3, 3.7, and 5.3 Hz). The directions of maximum amplification are not consistent across the array for these frequencies and the spatial pattern is complex (see Fig. 6). Interpolated maps of SRSR at selected frequencies are presented in Fig. 6 for both sites. Clear spatial trends are present for the first SRSR peaks (Randa: 2.3 Hz – 225°, 3.1 Hz – 135°; Walkerschmatt: 1.6 Hz – 120°). On the other hand, the spatial pattern is complex for other SRSR peaks (especially at Walkerschmatt).

ARRAY PROCESSING OF AMBIENT VIBRATIONS

Small-aperture seismic arrays have been widely used for characterization of the shear wave velocity structure in the shallow crust (<1 km). The method is particularly useful in layered soil media, where dispersive surface waves dominate the noise wavefield. The frequency-wavenumber (f-k) method is commonly used to retrieve phase velocity dispersion curves of surface waves, which are used in the inversion of velocity structure. The aim of f-k processing applied in the present work was to identify waves propagating across the array. In this study, we applied the high-resolution (Capon, 1969) f-k power spectral estimate method (so-called beamforming method), as implemented by Wathelet *et al.* (2008). Recorded time series were divided into overlapping windows of 100 s duration. A consecutive set of narrow-band filters (characterized by central frequencies) were applied to trace the frequency dependence. Wavenumber power spectra were then estimated for each time window and frequency band, and the location of the strongest peak in the spectrum was identified. Finally, an apparent velocity was calculated.

Results

We performed *f-k* analysis on recordings obtained at Walkerschmatt on Array 2 (yellow stations in Fig. 2), since the geometry of Array 1 (red stations in Fig. 2) was almost linear with a strongly asymmetric response. We focused on a subset of stations consisting of WAL201, WAL202, WAL203, WAL204, and WAL206, located in the area of the slope near the cliff face and delimited by a distinct surface crack. Horizontal components of recordings were rotated by 120° as in the previous analysis of site-to-reference spectral ratios. High-resolution *f-k* estimates of apparent velocities for the 120°-component are plotted in Fig. 8. Note the sharp increase in apparent velocity centered at ~ 1.6 Hz (red dashed line), which was identified as a potential fundamental frequency of the slope instability from SRSR analysis. The apparent velocities of these signals do not drop below 4 km/s in the narrow band (1.4-1.7 Hz) for any time window, and most of the points lie in the interval between 6 and 30 km/s. Although, all points picked below 3 Hz are beyond the resolution limit of the array, the observed increase in apparent velocities is not artificial (as shown in Burjanek *et al.*, 2011). Summarizing, observed apparent velocities of 6-30 km/s indicate that ground motion is generally in-phase at 1.6 Hz within the array. Although such high apparent velocities may indicate vertically-propagating plane waves, this is not an entirely plausible interpretation in our case. The apparent velocities drop dramatically in the frequency band between 1.6 and 2 Hz (Fig. 7), and such strong dispersion is not realistic in the case of body waves.

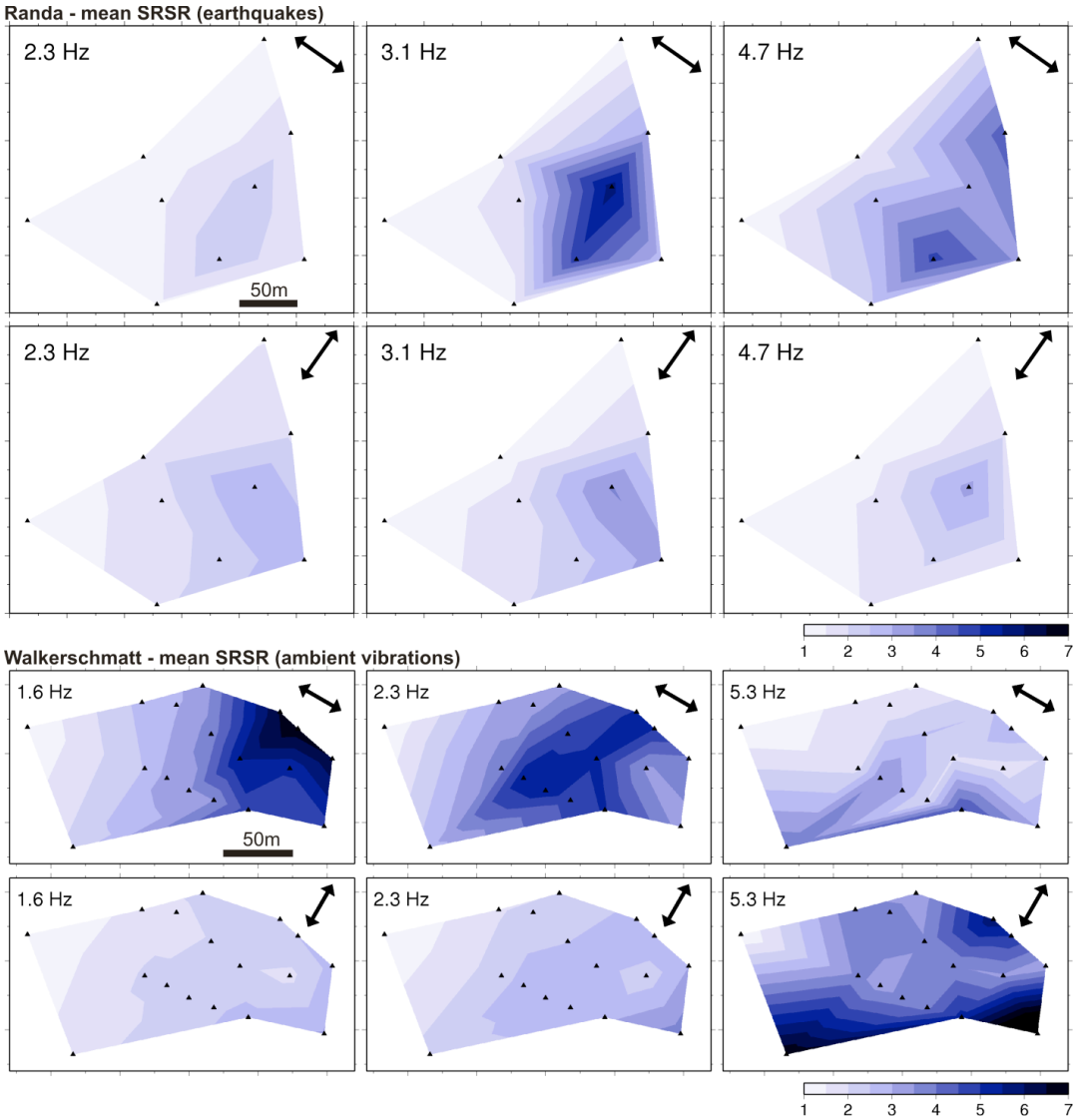

Fig. 6. Interpolated maps of site-to-reference spectral ratios (SRSR) for both Randa (based on earthquake recordings of geophone array; top) and Walkerschmatt (based on noise recordings; bottom) at different frequencies. SRSR are presented for two horizontal components depicted by black double-headed arrows (Walkerschmatt: 120° and 210° azimuths; Randa: 135° and 225° azimuths).

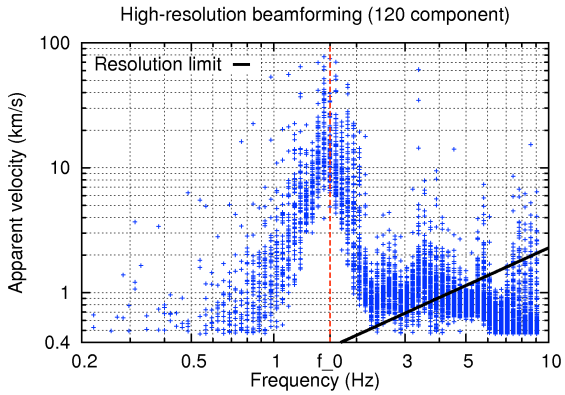

Fig. 7. Apparent velocities estimated by picking maxima in the wavenumber plane. The resolution limit estimated from the array response function is plotted by the black solid line. The fundamental frequency f_0 identified by polarization and SRSR analysis is shown as a dashed red line.

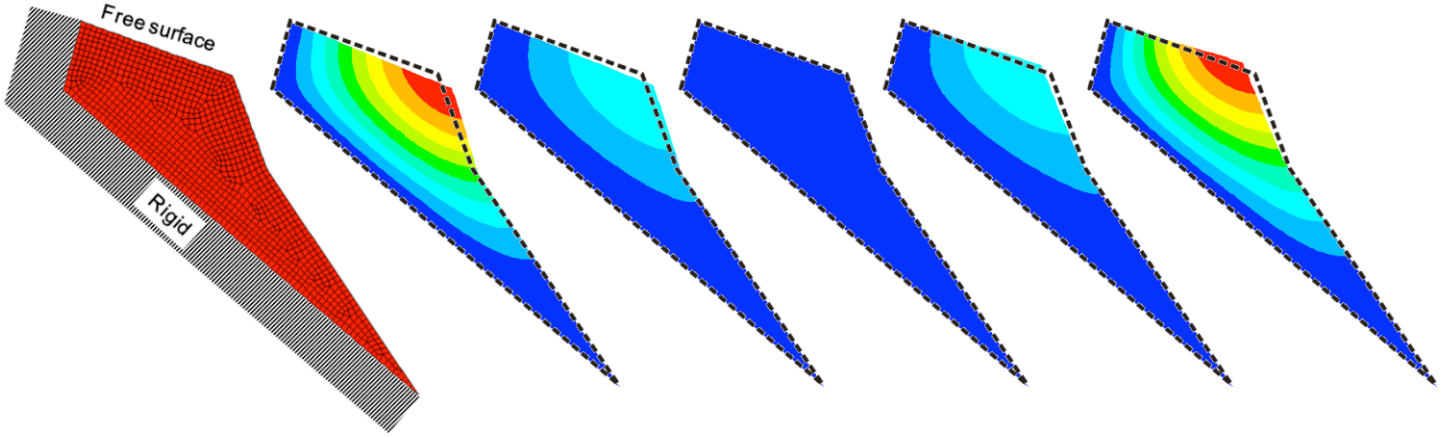

Fig. 8. Simplified 2D model of the Randa site implemented in ANSYS, and results of normal mode simulation. The finite element mesh and sketch of boundary conditions are presented in the first figure at left. Five snapshots of the deformed body represent the fundamental mode shape. Magnitude of the normalized horizontal displacement is indicated by the color. Black dashed line represents the undeformed shape of the body.

DISCUSSION

An increasing number of studies have reported directional site effects in areas of pronounced topography (e.g., Pischiutta *et al.*, 2010; Panzera *et al.*, 2011), and in some cases in association with potential landslides (Del Gaudio and Wasowski, 2011; Moore *et al.*, 2011). Briefly summarizing our main observations: 1) Ambient vibrations are strongly polarized at certain frequencies in the unstable areas. 2) Ground motion in the unstable portion of the slopes is relatively amplified in specific orientations with respect to stable area. The first peak in observed SRSRs is at the same frequency f_0 in the same direction at all stations. This direction is perpendicular to cracks observed at the ground surface. 3) The relative amplification at f_0 varies smoothly across the instability. 4) Ground motion is in-phase at f_0 (not yet verified at the Randa site). The preceding attributes are typical for normal mode vibration of sedimentary basins (Bard and Bouchon, 1985; Steimen *et al.*, 2003, Roten *et al.*, 2006), which is analogous to free oscillations of the Earth. We suggest here that the unstable rock mass may be viewed as a volume of effectively reduced elastic moduli (damaged rock with air-filled voids). The boundary between heavily fractured and more intact rock mass then presents a contrast in seismic impedance, which traps incoming waves. This results in the development of standing waves (normal mode vibration). Excitation of normal mode vibration by weak motions results in local site amplification factors of up to 7 within the unstable area with respect to the reference station on presumably stable ground. Such strong relative amplification can not be explained by topographic site effects alone. We next provide a simplified numerical model that can partially explain some of the observed ground motion features.

Numerical model

A simplified 2D elastic model was constructed to simulate normal mode motion of a body, which has the same shape as the unstable rock volume at the Randa instability (Fig. 8). The geometry of the unstable body was adapted from Willenberg *et al.* (2008), and the material in the body was assumed to be homogeneous and isotropic. A zero-displacement boundary condition was assumed at boundary between damaged and intact rock. The remaining boundary was assumed to be traction-free (free surface). The zero-displacement boundary condition at the bottom of the model substantially simplifies the solution, however may not be fully realistic. On the other hand, it is sufficient for first estimation of the resonant frequencies, assuming the existence of an impedance contrast between damaged and compact rock masses (Jiang and Kuribayashi, 1988; Paolucci, 1999). Finite-element simulation (ANSYS software package) was applied to solve the elastodynamic equation assuming a 2D medium and in-plane deformation. More specifically, we were seeking a solution for normal-mode shapes and Eigen-frequencies. We found through trial-and-error that a shear wave velocity of 900 m/s for the damaged rock mass (assuming Poisson's ratio = 0.2 and density = 2700 kg/m^3) reproduced the observed fundamental frequency of 3.1 Hz. The obtained value of shear wave velocity is not unrealistic for the damaged rock at Randa, as Spillmann *et al.* (2007) determined longitudinal velocity of 500 m/s close to the surface in the unstable area. The shape of the fundamental mode is represented by snapshots of the deformed body in Fig. 8. The maximum horizontal displacement occurs in the region of maximum instability thickness, as expected and observed.

Numerical simulation presented above is completely analogous to the simulation of normal modes in sedimentary basins (e.g., Bard and Bouchon, 1985). However, in real case, there is a fundamental difference in comparison to sedimentary basins. The specific polarization of the basin normal modes has its origin in basin geometry. For example in 2D analyses, ground motion can be separated

into SH and P-SV contributions with respect to the axis of the basin (Bard and Bouchon, 1985), where SH normal modes are polarized parallel to the valley axis and are perpendicular to P-SV modes. The strong directional site response observed in the present work, on the other hand, is likely caused by the fractured nature of the medium. The relationship between polarization and mapped fractures is apparent in Figs. 2 and 4. Predominant polarization of ambient noise at f_0 is perpendicular to observed surface cracks. We suggest that material within the unstable part of the rock slope is weakened by the cumulative effect of numerous parallel cracks, many of which can be observed at the surface. Since the cracks have a preferred orientation sub-perpendicular to the direction of slope displacement, effective anisotropy in rock mass moduli arises. Specifically, we suggest that the bulk stiffness of the fractured rock mass drops significantly in the direction perpendicular to the trace of tension cracks. We do not relate such an effect to inherent seismic anisotropy of the rock (e.g., due to micro-fracturing), but rather to the systematic orientation of open macro-fractures, which are common in deep-seated rock slope instabilities. This explanation is supported by recent numerical modeling of earthquake-induced ground motion at the Randa rock slope performed by Moore *et al.* (2011).

CONCLUSIONS

Measurements presented in this paper support the hypothesis that ambient vibration of large, unstable rock slopes are dominated by normal mode motion. Although the results presented here were obtained using seismic arrays, polarization analysis could be performed with single-station noise measurements (point by point). The density of measurement points is critical for correct interpretation of the seismic response. Strong directional amplification was linked to the internal structure of the slope, specifically to systematic fracture opening caused by slope movement, rather than topography. Complexity of the ground motion above the fundamental frequency further emphasizes the strong influence of subsurface internal structure. The resolved fundamental frequency of the slope instabilities could be monitored in the future (e.g. with a single seismic station) in order to asses any potential temporal changes related to internal damage that may precede failure (as in Lévy *et al.*, 2010). We emphasize that the slopes may behave differently under strong shaking (high-strain motion).

ACKNOWLEDGEMENTS

We thank Thomas Spillmann and Hansruedi Maurer for access to previously recorded seismic data from Randa. This research is funded in part by the Competence Center for Environment and Sustainability (CCES) of the ETH Domain, and by the Swiss National Science Foundation. Wavelet software was provided by C. Torrence and G. Compo, and is available at: http://paos.colorado.edu/research/wavelets/. Some figures in this article were made using Generic Mapping Tools (GMT) 4 by Wessel and Smith (1998).

REFERENCES

Andrews, D.J. [1986], "Objective determination of source parameters and similarity of earthquakes of different size", *Earthquake Source Mechanics*, ed. S. Das et al., Washington, DC: American Geophysical Union, pp. 259-268.

Bard, P.-Y., and M. Bouchon [1985], "The two-dimensional resonance of sediment-filled valleys", Bull. Seismol. Soc. Am., Vol. 75, pp. 519-541.

Borcherdt, R.D. [1970], "Effects of local geology on ground motion near San Francisco Bay", Bull. seism. Soc. Am., Vol. 60, pp. 29–61.

Burjanek, J., G. Stamm, V. Poggi, J.R. Moore, and D. Fäh [2010], "Ambient vibration analysis of an unstable mountain slope", Geophys. J. Int., Vol. 180, pp. 820-828.

Burjanek, J., J.R. Moore, F.X. Yugsi Molina, and D. Fäh [2011], "Instrumental evidence of normal mode rock slope vibration", submitted to Geophys. J. Int.

Capon, J. [1969], "High resolution frequency wavenumber spectrum analysis", Proc. IEEE, Vol. 57, pp. 1408-1418.

Danneels, G., C. Bourdeau, I. Torgoev, and H.-B. Havenith [2008], "Geophysical investigation and dynamic modelling of unstable slopes: case-study of Kainama (Kyrgyzstan)", Geophys. J. Int., Vol. 175, pp. 17–34.

Del Gaudio, V., and J. Wasowski [2007], "Directivity of slope dynamic response to seismic shaking", Geophys. Res. Lett., Vol. 34, L12301, doi:10.1029/2007GL029842.

Del Gaudio, V., and J. Wasowski [2011], "Advances and problems in understanding the seismic response of potentially unstable slopes", Engineering Geology, in press, doi:10.1016/j.physletb.2003.10.071.

Fäh, D., D. Giardini, P. Kästli, N. Deichmann, M. Gisler, G. Schwarz-Zanetti, S. Alvarez-Rubio, S. Sellami, B. Edwards, B. Allmann, F. Bethmann, J. Wössner, G. Gassner-Stamm, S. Fritsche, and D. Eberhard [2011], "*ECOS-09 Earthquake Catalogue of Switzerland Release 2011. Report and Database. Public catalogue, 17.4.2011*." Swiss Seismological Service ETH Zürich, Switzerland, Report SED/RISK/R/001/20110417.

Fritsche, S., D. Fäh, M. Gisler, and D. Giardini [2006], "Reconstructing the Damage Field of the 1855 Earthquake in Switzerland: historical investigations on a well-documented event", Geophys. J. Int., Vol. 166, pp. 719-731.

Fritsche, S., and D. Fäh. [2009], "The 1946 Magnitude 6.1 Earthquake in the Valais: Site-Effects as Contributor to the Damage", Swiss J. Geosci., Vol. 102, pp. 423-439.

Fritsche, S., M. Gisler, G. Schwarz, D. Fäh, and P. Kästli [2010], "*Historical Earthquakes in the Valais, COGEAR deliverable 1a.2.1*", Swiss Seismological Service, Zürich, Switzerland, Report SED/COGEAR/R/002/20100110.

Gischig, V., F. Amann, J.R. Moore, S. Loew, H. Eisenbeiss, and W. Stempfhuber [2011], "Composite rock slope kinematics at the current Randa instability, Switzerland, based on remote sensing and numerical modeling", Engineering Geology, Vol. 118, pp. 37-53.

Irikura, H., and T. Kawanaka [1980], "Characteristics of microtremors on ground with discontinuous undergone structure", Bull. Disas. Prev. Res. Inst., Vol . 30, pp. 81–96.

Jiang, T., and E. Kuribayashi [1988], "The three-dimensional resonance of axisymmetric sediment-filled valleys", Soils and Foundations, Vol. 28, pp. 130-146.

Keefer, D.K. [2002], "Investigating landslides caused by earthquakes – a historical review", Surveys in Geophysics, Vol. 23, pp. 473–510.

Konno, K., and T. Ohmachi [1998], "Ground-Motion Characteristics Estimated from Spectral Ratio between Horizontal and Vertical Components of Microtremor", Bull. Seism. Soc. Am., Vol. 88, pp. 228–241.

Lévy, C., L. Baillet, D. Jongmans, P. Mourot, and D. Hantz [2010], "Dynamic response of the Chamousset rock column (Western Alps, France)", J. Geophys. Res., Vol. 115, F04043, doi:10.1029/2009JF001606.

Marano, K.D., D.J. Wald, and T.I. Allen [2010], "Global earthquake casualties due to secondary effects: a quantitative analysis for improving rapid loss analyses", Nat. Hazards, Vol. 52, pp. 319-328.

Moore, J.R., V. Gischig, J. Burjanek, S. Loew, and D. Fäh [2011], "Site effects in unstable rock slopes: dynamic behavior of the Randa instability (Switzerland)", accepted for publication in Bull. Seismol. Soc. Am.

Panzera, F., G. Lombardo, and R. Rigano [2011], "Evidence of Topographic Effects through the Analysis of Ambient Noise Measurements", Seism. Res. Lett., Vol. 82, pp. 413-419.

Paolucci, R., [1999], "Shear resonance frequencies of alluvial valleys by Rayleigh's method", Earthquake Spectra, Vol. 15, pp. 503-521.

Pischiutta, M., G. Cultrera, A. Caserta, L. Luzi, and A. Rovelli [2010], "Topographic effects on the hill of Nocera Umbra, central Italy", Geophys. J. Int., Vol. 182, pp. 977–987.

Roten, D., C. Cornou, D. Fäh, and D. Giardini [2006], "2D resonances in Alpine valleys identified from ambient vibration wavefields", Geophys. J. Int., Vol. 165, pp. 889–905.

Roten, D., and D. Fäh [2007], "A combined inversion of Rayleigh wave dispersion and 2-D resonance frequencies", Geophys. J. Int., Vol. 168, pp. 1261-1275.

Spillmann, T., H. R. Maurer, H. Willenberg, K. F. Evans, B. Heincke, and A. G. Green [2007], “Characterization of an unstable rock mass based on borehole logs and diverse borehole radar data”, Journal of Applied Geophysics, Vol. 61, pp. 16-38.

Steimen S., D. Fäh, F. Kind, C. Schmid, and D. Giardini, [2003], “Identifying 2-D resonance in microtremor wave fields”, Bull. Seism. Soc. Am., Vol. 93, pp. 583–599.

Torrence, C., and G. P. Compo [1998], “A practical guide to wavelet analysis”, Bull. Amer. Meteor. Soc., Vol. 79 , pp. 61-78.

Vidale, J. E. [1986], “Complex polarisation analysis of particle motion”, Bull. Seismol. Soc. Am., Vol. 76, pp. 1393–405.

Wathelet, M., D. Jongmans, M. Ohrnberger, and S. Bonnefoy-Claudet [2008], “Array performances for ambient vibrations on a shallowstructure and consequences over Vs inversion”, J. Seismol., Vol. 12, pp. 1–19.

Wessel, P., and W. H. F. Smith [1998], “New, improved version of the Generic Mapping Tools released”, EOS Trans. AGU, Vol. 79, pp. 579.

Willenberg, H., S. Loew, E. Eberhardt, K. F. Evans, T. Spillmann, B. Heincke, H. Maurer, and A. G. Green [2008], “Internal structure and deformation of an unstable crystalline rock mass above Randa(Switzerland): Part I-Internal structure from integrated geological and geophysical investigations”, Engineering Geology, Vol. 101, pp. 1-14.

Yugsi Molina, F.X. [2010], “Structural control of multi-scale discontinuities on slope instabilities in crystalline rock (Matter valley, Switzerland)”, Ph.D. Thesis, Engineering Geology, ETH Zurich, Switzerland.